Progress In Electromagnetics Research C, Vol. 44, 41–53, 2013

INTEGRATED ULTRA-WIDEBAND PLANNAR MONOPOLE WITH CYLINDRICAL DIELECTRIC RESONATOR ANTENNAS

Yong-Feng Wang[1, 2, *], Shu Liu[1], Tayeb A. Denidni[2], Qing-Sheng Zeng[3], and Gao Wei[1]

[1]School of Electronics and Information, Northwestern Polytechnic University, Xi'an, Shaanxi 710129, China

[2]INRS-EMT, University of Quebec, Montreal, QC H5A 1K6, Canada

[3]Wireless Technologies Branch, Communications Research Centre Canada, Ottawa, Ontario K2H 8S2, Canada

Abstract—An ultra-wideband (UWB) planar monopole antenna integrated with a narrow-band (NB) cylindrical dielectric resonator antenna (DRA) is presented. The proposed antenna consists of a UWB monopole excited by a coplanar waveguide (CPW) transmission line, acting as a ground for a DRA excited by a slot. The mode $HEM_{11\delta}$ is excited in the NB DRA. To validate the concept of integration, an antenna is fabricated and measured. The measured results demonstrate that the UWB antenna provides a 2 : 1 voltage standing wave ratio (VSWR) bandwidth for 3.05–11 GHz, integrated with a dual-band NB antenna. Moreover, the two ports have the same polarization and a reasonable isolation (less than −10 dB) between each other. This is a promising candidate for applications in cognitive radio, where the UWB antenna can be used for spectrum sensing and the NB antenna for communication operation.

1. INTRODUCTION

Dielectric resonator antennas (DRAs) have received much attention as efficient radiators in recent years [1]. They can maintain high radiation efficiency, even at millimeter-wave frequencies due to low surface wave losses and minimal conductor losses. Moreover, the remarkable broad and ultra wideband (UWB) features offered by

Received 9 July 2013, Accepted 12 September 2013, Scheduled 13 September 2013

* Corresponding author: Yong-Feng Wang (yongfeng.wang@emt.inrs.ca).

DRAs make them as potential candidates for UWB systems [2–9]. The intensive investigations on UWB DRAs have been pursued and published. Using hybrid configurations, several monopole-DRAs have been studied, which are constructed by a vertical monopole antenna loaded with a ring-shaped dielectric resonator (DR) around in the horizontal plane [4–8]. Recently, a combination of broadband planar monopole and a rectangular DRA has been reported, which has a bandwidth from 3.06 to 10.6 GHz [9].

In recent years, the underutilization of the frequency spectrum has inspired the use of reconfigurable radio concepts, such as cognitive radio (CR) [10]. In category A of CR systems, two antennas were used. A wideband antenna to feed a receiver for spectrum sensing and a narrow band (NB) antenna to feed the front end, which can be tuned to the second band [11]. A number of antennas that integrated wideband and NB antennas have successfully been designed for this application [12–15]. They are mainly based on the planar monopole and slot antennas.

In this paper, we propose a new integrated DRA. It consists of three parts: a cylindrical DR, a circular planar patch combined with a rectangular patch fed by a coplanar waveguide (CPW) (Port 1), and a slot fed by a microstrip line (Port 2). For Port 2, the microstrip line is printed on the reverse side of the substrate in order to use its ground plane for the UWB antenna. The planar monopole can excite several modes in the DR, which broaden the bandwidth. The slot on the ground can excite one HEM mode, which displays NB characteristic. The two ports are collinear to ensure that the sensing can measure interferences in the same polarization as the operation.

This paper is organized as follows. In Section 2, the integration method and design details are described, and simulation results are presented and discussed. In Section 3, a dual-band DRA instead of the NB DRA is proposed in Section 3. In this work, a prototype antenna was fabricated and measured, with which the antenna bandwidth and radiation pattern are investigated experimentally. The experimental results are provided and compared with simulated ones in Section 4. Our work is concluded in Section 5.

2. THE INTEGRATED WIDE-NARROWBAND ANTENNA

2.1. Integration Concept

When integrating multiple antennas into a limited space, the challenging design goal is to reduce the mutual coupling between these antennas. The integration concept of using a printed antenna

with a relatively large metallization area as a ground plane for an additional antenna has been proposed in [14]. Achieving adequate isolation between the two ports is one of the main issues in the design of integration. However, controlling the power coupled between the two ports is very challenging in closely spaced antennas.

The design flexibility offered by DRAs makes them suitable for many wireless applications [16–18]. Using a hybrid configuration, multi-modes can be easily excited in the DRA, such as fed by a planar patch. Thus UWB DRAs can be easily achieved. Meanwhile, each single mode of the DRA has a narrow-band characteristic. Due to these reasons, they are good candidates for the integration application. In addition, due to the three-dimensional structure and the unique electric field distribution of each mode, the mutual coupling between the two ports can be controlled more easily. Another advantage of using DRAs in the integration is that a multi-band antenna can be realized instead of a single narrow-band antenna due to their multi-mode characteristic.

2.2. UWB DRA Design

Broadband planar monopole antennas have received considerable attention due to their attractive advantages, such as ultra-wide frequency band, good radiation characteristic, simple structures, low cost and easy fabrication [19–21]. The typical shapes of these antennas are half-disc, circle, ellipse and rectangular. In addition, with the electromagnetic coupling between the feeding monopole and the dielectric resonator, UWB DRAs can be easily achieved. The proposed planar monopole is shown in Figure 1. A circular patch is designed for the UWB monopole with an additional rectangular patch for the

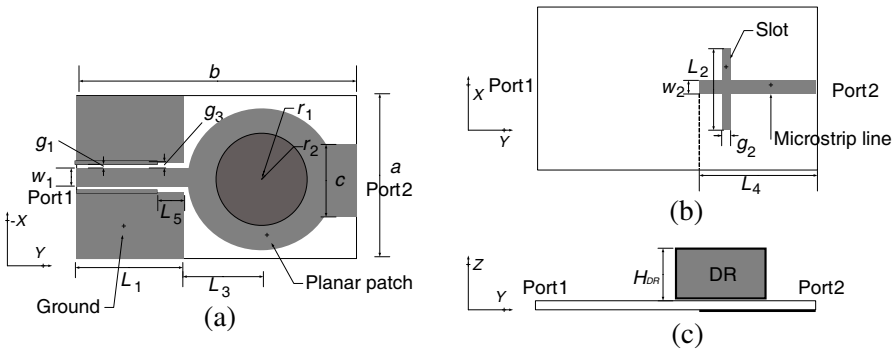

Figure 1. Geometry of the integrated DRA. (a) Top-view. (b) Back-view. (c) Side-view.

integration. The rectangular patch designed for the integration is not necessary for the UWB DRA, which should be large enough to insure that the edge effect on the input impedance of Port 2 can be negligible.

The overall size is $38 \times 25\,\text{mm}^2$. It is prototyped on Rogers RO4350B substrate with dielectric permittivity of 3.66, loss tangent of 0.004 and thickness of 0.762 mm. A $50\,\Omega$ CPW line with dimensions $w_1 = 3\,\text{mm}$, $g_1 = 0.2\,\text{mm}$ is employed to feed the UWB antenna. The ground plane and the DR are on the front surface of the substrate. In the ground for Port 1, the rectangular slot ($L_5 \times g_3$) creates a capacitive load to neutralize the inductive nature of the patch. The cylindrical DR is made of Rogers 6006 substrate with the dielectric permittivity of 6.15 and loss tangent of 0.003, with dimensions $r_2 = 8\,\text{mm}$, $H_{DR} = 10\,\text{mm}$. The configuration parameters are summarized in Table 1. The simulation was carried out using CST, and the simulated reflection coefficient (S_{11}) of the UWB DRA is shown in Figure 2. From this result, it can be seen that the proposed antenna provide an impedance bandwidth from 3.05 to 11.5 GHz.

Table 1. Final dimensions of the antenna.

parameter	b	a	L_1	L_2	L_3	L_4	L_5	w_1
mm	38	25	16	10	10.4	14.7	4.5	3
parameter	w_2	g_1	g_2	g_3	r_1	r_2	c	H_{DR}
mm	1.7	0.2	0.6	0.4	10	8	10	10

2.3. Integrated Antenna Design

The integrated antenna is shown in Figure 1. To ensure that the sensing can measure interferences in the same polarization as the operation, the two ports must be collinear. Therefore, the two ports are designed at the opposite sides of the substrate. Moreover, arranging the two ports at the opposite sides has the advantage of low mutual coupling. For the NB port (Port 2), the width of the feeding microstrip line is 1.7 mm, and its characteristic impedance is $50\,\Omega$. The DR is located on the center of the circular patch, as shown in Figure 1. The resonator frequency of the excited $\text{HEM}_{11\delta}$ mode of the proposed DRA is calculated by [1]

$$f_{\text{HEM}11\delta} = \frac{6.324}{\sqrt{\varepsilon_r + 2}} \left(0.27 + 0.36\frac{r}{h} + 0.02\left(\frac{r}{2h}\right)^2\right) \frac{4.7713}{r} \qquad (1)$$

where r and h are the radius and height of the cylindrical DRA, respectively. After calculation, the resonator frequency of mode

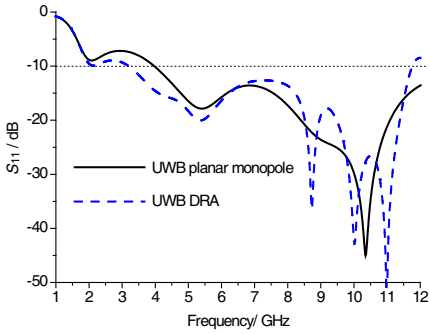

Figure 2. Simulated reflection coefficient of the UWB DRA.

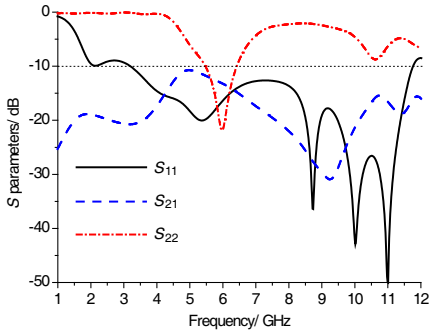

Figure 3. Simulated results of the integrated DRA.

$\text{HEM}_{11\delta}$ is 5.468 GHz. The length of the feeding slot is designed using the following formula [9]

$$f = \frac{c}{2L}\sqrt{\frac{2}{\varepsilon_{r1} + \varepsilon_{r2}}} \tag{2}$$

where c is the speed of light in vacuum, L the length of slot, and ε_{r1} and ε_{r2} are the relative permittivity of the substrate and DR, respectively. The width and position of the slot and the length of the feeding microstrip line are optimized.

Using CST software tool, the proposed antenna was simulated, and the simulated S_{11}, S_{22} and S_{21} are shown in Figure 3. The mode $\text{HEM}_{11\delta}$ is excited in Port 2, which can be confirmed by the electric field distribution of this frequency in the DR. The simulation resonator frequency of mode $\text{HEM}_{11\delta}$ is 5.7 GHz, which corresponds to the calculated result. We can see the mutual coupling is weak for the whole band. This is due to the three-dimensional structure and the unique electric-filed distribution of the mode $\text{HEM}_{11\delta}$. Figure 4 shows the calculated peak gain of the integrated antenna. Some degradation is inevitable for the integrated antenna. The gain increase of the UWB antenna at 9 GHz is due to the higher-mode of the DRA.

3. DUAL-BAND DRA DESIGN

The integrated antenna designed in Section 2 is successful. Using the same integration concept, a dual-band antenna can be also integrated with a UWB antenna. The only difference between the integrated dual-band antenna and the antenna in Section 2 is the cylindrical DR. The cylindrical DR for the dual-band is made of Rogers 6110 substrate

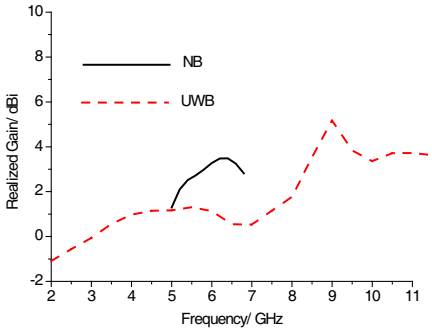

Figure 4. Simulated realized gain of the integrated DRA.

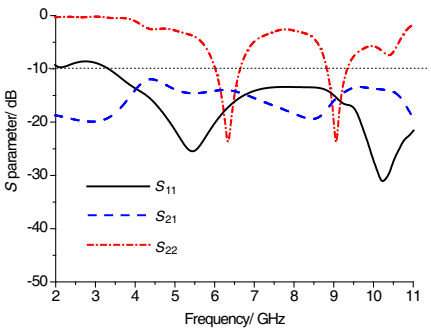

Figure 5. Simulated results of the proposed DRA.

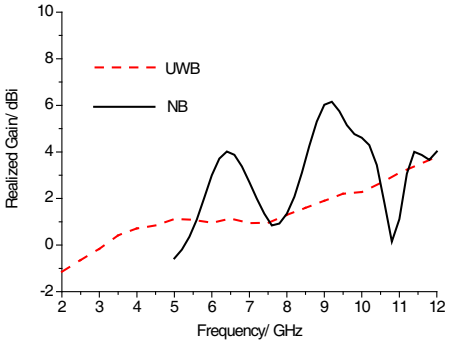

Figure 6. Simulated gain of the proposed DRA.

with the dielectric permittivity of 10.2 and loss tangent of 0.003, with dimensions $r_2 = 5.8\,\text{mm}$, $H_{DR} = 10\,\text{mm}$. The simulated S-parameters are shown in Figure 5. The mutual coupling is also less than $-10\,\text{dB}$ for the whole band. Figure 6 shows the calculated peak gain of the proposed antenna. It is seen that the peak gain of the UWB antenna is stable across the operating frequency range.

4. FABRICATION AND MEASUREMENT

To validate the simulated results, a prototype integrated DRA associated with the given parameters in Section 3 was fabricated and measured. The antenna performances in terms of bandwidth and radiation pattern were investigated numerically and experimentally. Figure 7 is the photograph of the fabricated UWB planar monopole antenna. Figure 8 plots the measured and simulated impedance

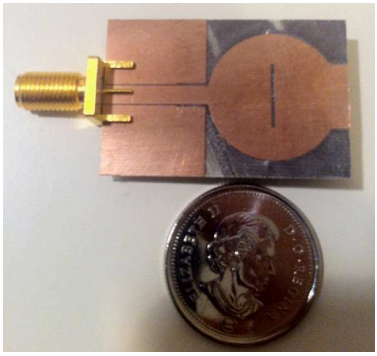

Figure 7. Photograph of the fabricated UWB planar monopole antenna.

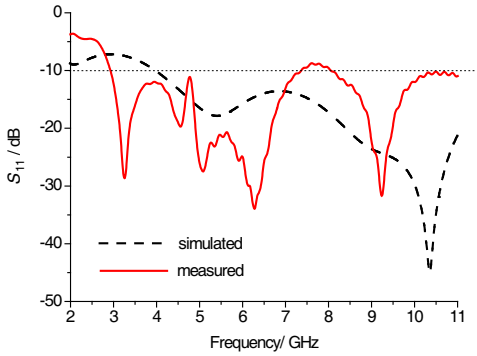

Figure 8. Measured S_{11} of the UWB planar monopole antenna.

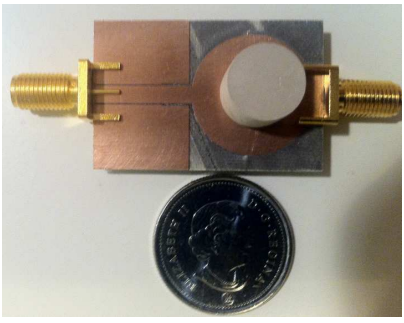

Figure 9. Photograph of the fabricated integration antenna.

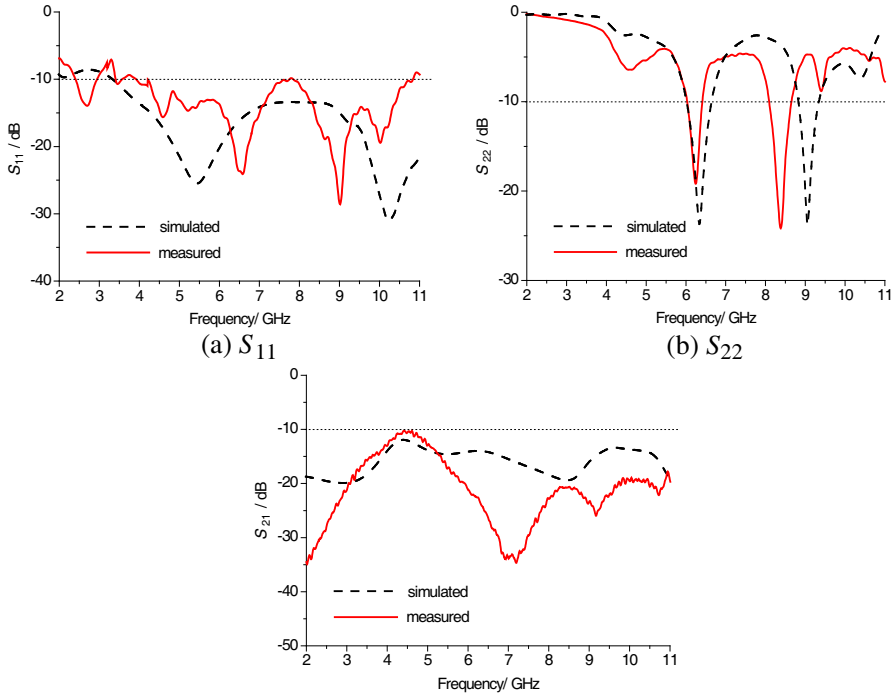

Figure 10. Measured S-parameters of the integration antenna.

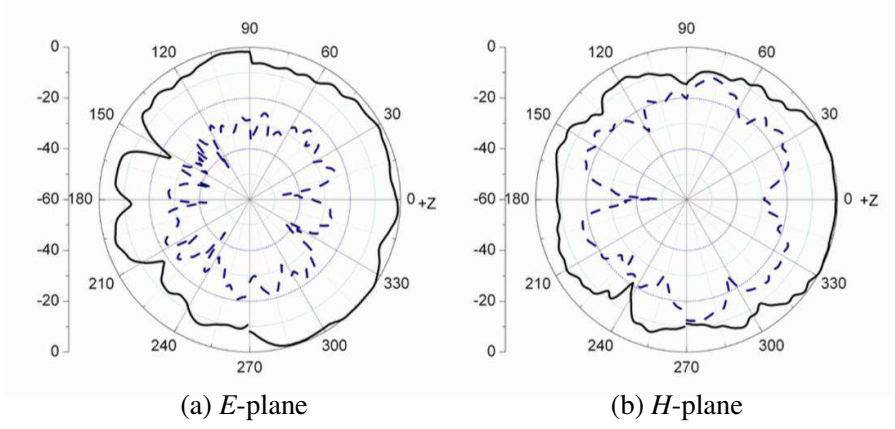

Figure 11. Radiation patterns for the narrow-band antenna at 6.2 GHz (solid: co-polarization; dot: cross-polarization).

bandwidth curves. The measured bandwidth covers the range from 3 to 11 GHz for VSWR < 2. Due to the fabrication imperfection and the influence of the SMA connector, some difference between the simulated and measured results is seen.

Figure 9 is the photograph of the fabricated integrated DRA. The DR is formed by stacking the material with superglue. In addition, the DR is adhered to the patch also with superglue. This provides a firm and solid bond. However, using different materials with low permittivity may lead to some impacts on the design results.

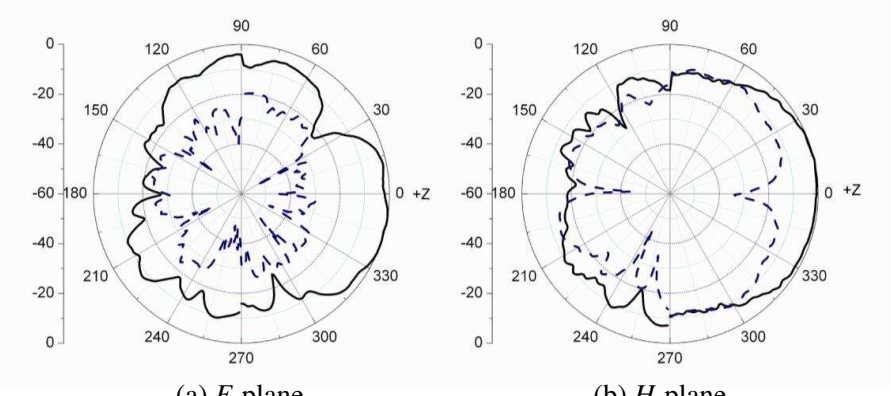

(a) *E*-plane (b) *H*-plane

Figure 12. Radiation patterns for the narrow-band antenna at 8.5 GHz (solid: co-polarization; dot: cross-polarization).

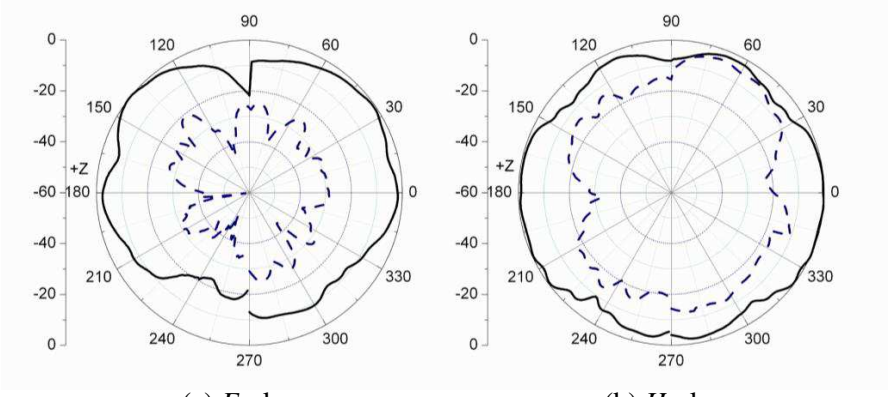

(a) *E*-plane (b) *H*-plane

Figure 13. Radiation patterns for the UWB antenna at 4 GHz (solid: co-polarization; dot: cross-polarization).

Therefore, to reduce the impacts, the superglue layer should be made as thin as possible. Figure 10 plots its measured and simulated S-parameters. The measured results demonstrate that a dual-band (5.9–6.3 GHz and 8.0–8.6 GHz) antenna is integrated with a UWB antenna with a reasonable isolation (less than −10 dB).

Figures 11 and 12 illustrate the measured radiation patterns in the yz-plane (E-plane) and the xz-plane (H-plane) of the fabricated antenna for the narrow-band antenna at 6.2 GHz and 8.5 GHz. It is clear from Figures 11 and 12 that the cross polarization levels are

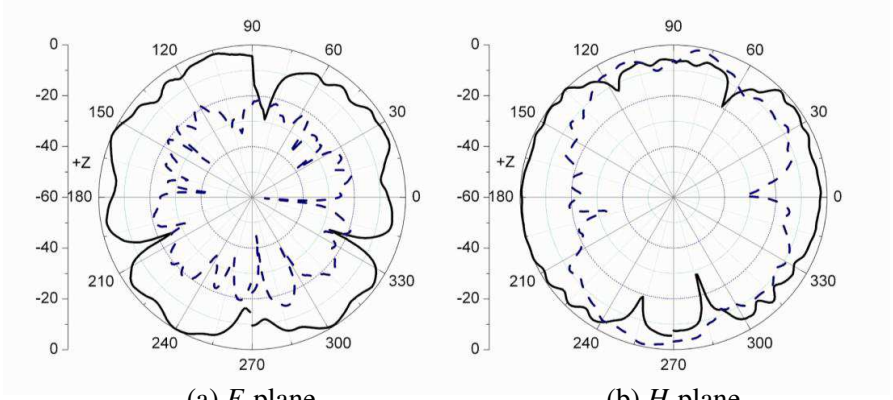

(a) E-plane (b) H-plane

Figure 14. Radiation patterns for the UWB antenna at 6 GHz (solid: co-polarization; dot: cross-polarization).

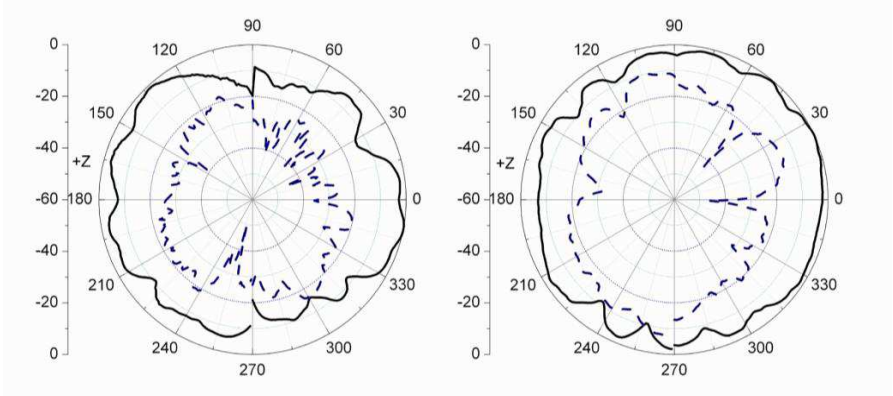

(a) E-plane (b) H-plane

Figure 15. Radiation patterns for the UWB antenna at 8 GHz (solid: co-polarization; dot: cross-polarization).

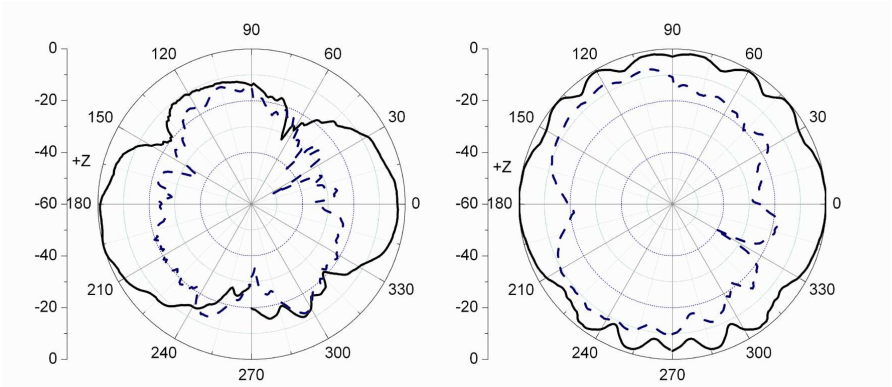

(a) *E*-plane (b) *H*-plane

Figure 16. Radiation patterns for the UWB antenna at 10 GHz (solid: co-polarization; dot: cross-polarization).

less than −30 dB in the direction of maximum radiation (Z-axis). The front-lobes and back-lobes were measured separately, so they are discontinuous.

Figures 13 to 16 illustrate the measured radiation patterns in the yz-plane (E-plane) and the xz-plane (H-plane) of the fabricated UWB antenna at different frequencies over the operation band. The radiation patterns are suitable for UWB applications.

5. CONCLUSION

A compact UWB antenna integrated with a NB antenna has been presented. This antenna provides two bandwidths: one is from 3.05 to 11.5 GHz and a second from 5.5 to 6.5 GHz. with the same polarization and a reasonable isolation. To validate the concept of integration, a UWB antenna integrated with a dual-band antenna was fabricated and measured. The results prove that UWB DRAs can be easily integrated with a narrow-band antenna. Using the same concept of integration, DRAs with other geometric structures than cylindrical ones can be also used in this antenna concept.

ACKNOWLEDGMENT

The authors would like to thank Rogers Corporation for providing the microwave substrate materials through the University Program. This work is supported by China Scholarship Council (CSC) (201206290106).

REFERENCES

1. Petosa, A. and A. Ittipiboon, "Dielectric resonator antenna: A historical review and the current state of the art," *IEEE Antennas Propag. Mag.*, Vol. 52, No. 5, 91–116, Oct. 2010.
2. Ahmed, O. M. H., A. R. Sebak, and T. A. Denidni, "Size reduction and bandwidth enhancement of a UWB hybrid dielectric resonator antenna for short range wireless communication," *Progress In Electromagnetics Research Letters*, Vol. 19, 19–30, 2010.
3. Aoutoul, M., N. Healey, J. Kiwan, F. Bourzeix, B. Lakssir, and M. Essaaidi, "A very small UWB dielectric resonator antenna for mobile and wireless communication systems," *PIERS Proceedings*, 102–105, Marrakesh, Morocco, Mar. 20–23, 2011.
4. Guha, D., Y. M. M. Antar, A. Ittipiboon, A. Petosa, and D. Lee, "Improved design guidelines for the ultra wideband monopole-dielectric resonator antenna," *IEEE Antennas Wirel. Propag. Lett.*, Vol. 5, 373–377, 2006.
5. Zivkovic, I., "Dielectric loading for bandwidth enhancement of ultra-wide band wire monopole antenna," *Progress In Electromagnetics Research C*, Vol. 30, 241–252, 2012.
6. Niroo-Jazi, M. and T. A. Denidni, "Experimental investigations of a novel ultrawideband dielectric resonator antenna with rejection band using hybrid techniques," *IEEE Antenna Wirel. Propag. Lett.*, Vol. 11, 492–495, 2012.
7. Ozzaim, C., "Monopole antenna loaded by a stepped-radius dielectric ring resonator for ultrawide bandwidth," *IEEE Antenna Wirel. Propag. Lett.*, Vol. 10, No. 1, 843–845, 2011.
8. Ozzaim, C., F. Ustuner, and N. Tarim, "Stacked conical ring dielectric resonator antenna excited by a monopole for improved ultrawide bandwidth," *IEEE Trans. Antennas Propag.*, Vol. 61, No. 3, 1435–1438, 2013.
9. Denidni, T. A. and Z. Weng, "Hybrid ultrawideband dielectric resonator antenna and band-notched designs," *IET Microw. Antennas Propag.*, Vol. 5, No. 4, 450–458, 2011.
10. Mitola, J. and G. Q. Maguire, "Cognitive radio: Making software radios more personal," *IEEE Personal Commun.*, Vol. 6, 13–18, Aug. 1999.
11. Hall, P. S., P. Gardner, and A. Faraone, "Antenna requirement for software defined and cognitive radios," *Proceedings of the IEEE*, Vol. PP, No. 99, 1–9, 2012.
12. Ghanem, F., P. S. Hall, and J. R. Kelly, "Two port frequency reconfigurable antenna for cognitive radios," *IET Electron. Lett.*,

Vol. 45, No. 11, 534–535, May 2009.

13. Kelly, J. R., P. Song, P. S. Hall, and A. L. Borja, "Reconfigurable 460 MHz to 12 GHz antenna with integrated narrowband slot," *Progress In Electromagnetics Research C*, Vol. 24, 137–145, Sep. 2011.
14. Ebrahimi, E., J. R. Kelly, and P. S. Hall, "Integrated wide-narrowband antenna for multi-standard radio," *IEEE Trans. Antennas Propag.*, Vol. 59, No. 7, 2628–2635, Jul. 2011.
15. Augustin, G. and T. A. Denidni, "An integrated ultra wideband/narrow band antenna in uniplanar configuration for cognitive radio systems," *IEEE Trans. Antennas Propag.*, Vol. 60, No. 11, 5479–5484, Nov. 2012.
16. Khalily, M., M. K. A. Rahim, and A. A. Kishk, "Bandwidth enhancement and radiation characteristics improvement of rectangular dielectric resonator antenna," *IEEE Antenna Wirel. Propag. Lett.,* Vol. 10, 393–395, 2011.
17. Yan, J. and J. T. Bernhard, "Design of a MIMO dielectric resonator antenna for LTE femtocell base station," *IEEE Trans. Antennas Propag.*, Vol. 60, No. 2, 438–444, 2012.
18. Fakhte, S., H. Oraizi, and M. H. Vadjed-Samiei, "A high gain dielectric resonator loaded patch antenna," *Progress In Electromagnetics Research C*, Vol. 30, 147–158, 2012.
19. Kim, D.-O., N.-I. Jo, H.-A. Jang, and C.-Y. Kim, "Design of the ultrawideband antenna with a quadruple-band rejection characteristics using a combination of the complementary split ring resonators," *Progress In Electromagnetics Research*, Vol. 112, 93–107, 2011.
20. Zhu, F., S. Gao, A. T. S. Ho, C. H. See, R. A. Abd-Alhameed, J. Li, and J. Xu, "Design and analysis of planar ultra-wideband antenna with dual band-notched function," *Progress In Electromagnetics Research,* Vol. 127, 523–536, 2012.
21. Xie, M., Q. Guo, and Y. Wu, "Design of a miniaturized UWB antenna with band-notched and high frequency rejection capability," *Journal of Electromagnetic Waves and Applications*, Vol. 25, Nos. 8–9, 1103–1112, 2011.